Preprint Title Controlled Release of Doxorubicin from pH-responsive Cockle Shell-derived Nanoparticle and its Pharmacokinetics in Dogs

Authors Abubakar Danmaigoro, Gayathri T. Selvarajah, Mohd Hezmee Mohd Noor, Rozi Mahmud, Wun C. How, Ahmed Hamidu and Zuki Abu Bakar

Publication Date 02 Sep 2019

Article Type Full Research Paper

ORCID® iDs Abubakar Danmaigoro - https://orcid.org/0000-0002-0833-6380

Controlled Release of Doxorubicin from pH-responsive Cockle Shell-derived Nanoparticle and its Pharmacokinetics in Dogs

Abubakar Danmaigoro[1,6]; Gayathri Thevi Selvarajah[2]; Mohd Hezmee Mohd Noor [1]; Rozi Mahmud[3]; Wun Chee How[4]; Ahmed Hamidu[5] Zuki Abu Bakar[1*],

[1]Department of Veterinary Preclinical Sciences, Faculty of Veterinary Medicine, Universiti Putra Malaysia, 43400 Serdang, Selangor Darul Ehsan, Malaysia.
[2]Department of Veterinary Clinical Sciences, Faculty of Veterinary Medicine, Universiti Putra Malaysia, 43400 Serdang, Selangor Darul Ehsan, Malaysia.
[3]Department of Imaging, Faculty of Medicine and Health Science, Universiti Putra Malaysia, 43400 Serdang, Selangor Darul Ehsan, Malaysia.
[4]Faculty of Pharmacy, MAHSA Selangor, Darul Ehsan, Malaysia [5]Institute of Bioscience, Universiti Putra Malaysia, 43400 Serdang, Selangor Darul Ehsan, Malaysia. [6]Department of Veterinary Anatomy, Faculty of Veterinary Medicine, Usmanu Danfodiyo University, P.M.B 2346, Sokoto-Nigeria

***Corresponding Author:** Prof. Dr. Md Zuki Abu Bakar
Department of Veterinary Preclinical Science,
Faculty of Veterinary Medicine,
Universiti Putra Malaysia
43400, Serdang,
Selangor, Darul Ehsan, Malaysia.
E-mail: zuki@upm.edu.my
Tel: +60196046659

Abstract

Stimuli-responsive cockleshell derived nanocarrier (CSNP) have huge potential in drug targeted delivery. They can be employed for targeted site-specific drug delivery due to its responsive nature to stimuli such as change in pH which minimizing its systemic off-targeted effect to due to excessive releases of doxorubicin. We use a simple top-down method to synthesis CSNP carrier from biological waste of cockleshell, which were negatively charged with higher loading capacity when conjugated with DOX. This study is aimed at demonstrating the *in vitro* release mechanism of DOX from CSNP under the influence of change in pH and to develop a bioanalytical method for pharmacokinetics of the synthesized CSNP-DOX in dogs. Apart from drug release kinetic of CSNP evaluation, a high-performance liquid chromatography bioanalytical method was developed and validated for the pharmacokinetics of CSNP-DOX determination. Six dogs were divided into two groups to receive CSNP-DOX and free DOX 30 mg/m^2 i.v respectively. At predetermined time interval, blood was sampled and processed for DOX concentration. The CSNP-DOX with high encapsulation efficiency and a mean diameter of 34.0 ± 3.4 nm was used. The *in vitro* release profiles demonstrated by DOX release from CSNP-DOX-loaded were pH dependent in nature which follows a Higuchi mathematical model equation. Pharmacokinetic parameters were determined with an excellent bioanalytical method having high extraction yield and linearity of 89.87% and 0.997. CSNP-DOX increases the $t_{1/2}$ and AUC_{0-t} of DOX as compared to dogs given free DOX. Our data further reveal a sustained release of DOX from CSNP under the influence of change in pH. However, we developed a rapid bioanalytical method for cumula al model. Based on these novel results, CSNP reveal to have promising ability to prolong release of DOX in circulation which tends

to reduce cytotoxic DOX release quantification which was further expressed on kinetic mathematic

Keywords: pH-triggered release; CSNP-DOX; Bioanalytical assay; Pharmacokinetics; Dog

1. Introduction

Stimuli-responsive nanocarriers are known to have the ability to improve the therapeutic index of chemotherapeutics upon delivery [1]–[3]. In recent times, stimuli-responsive nanocarriers have received significant attention in pharmaceutical industries due to the fact that, tumour microenvironment has different pH as when compared to the surrounding normal tissues, paving way for targeted drug delivery [3], [4]. Stimuli-responsive nanocarriers has great potentials in maintaining drugs therapeutic concentration in circulation since higher concentration of chemotherapuetics are associated with cytotoxicity due to early peak concentration which is followed by linear release in circulation [5]–[8]. Targeted drug delivery strategies direct drug to specific pathological sites with minimal or no adverse effect on the surrounding normal cells and tissues by altering the pharmacokinetic parameters of the drugs [9]. Currently, so many novel stimuli-responsive nanocarriers are designed for anticancer delivery, although many of them encountered numerous setbacks ranging accumulative toxicity in tissue leading to their decline in clinical application [10]. In this regard, Cockleshell calcium carbonate nanoparticles (CSNP) could serve as smart nanocarriers due to its facile pH-responsive trigger release of drugs in weak acidic microenvironment. These property have drawn the attention of research in the field of drug and gene delivery towards improve drug therapeutic index [11]. CSNP can be used as drug carrier for

the delivery of chemotherapeutic agents in order to improve the anti-cancer potency of the agents and reduces systematic off-targeted effects.

Doxorubicin (DOX) is a potent chemotherapeutic drug currently used for the treatment of metastatic cancers in dogs [12], [13]. However, due to the lack of cell specificity, heterogeneous blood supply and interstitial pressure in solid tumours prevent drug dispersion and penetration into the tumour thus, leading to its decline in clinical application [5], [13], [14]. Moreorever, the mechanism of toxicity is complex, so very difficult to pinpoint single pathway due to the involvement of multiple processes [15]. Although, lipid peroxidation, oxygen free radical release by oxidative reaction within cell mitochondria are famous in induced tissue injury [16]. Moreover, the bioavailability of DOX at the tumour site is often poor due tumour interstitial pressure, heterogeneous blood supply network hindering DOX penetration to tumour site, thus, necessitate additional doses, consequently leading to tissue damage due early concentration peak in circulation [17]. It is important to state that dogs are used as translational model in drug development and discovery, since they possess similar anatomical and physiological status with other mammals as compared to small laboratory rodents [18]. Hence, they serve as the most preferred model for therapeutic evaluation of new drugs [19].

In a way to remedy the problems associated with DOX is by encapsulating it on a nanocarriers with distinct physicochemical properties which can alter the pharmacokinetic profile and bioavailability of DOX, thereby modulating the drug's therapeutic efficacy and safety [20], [21]. For instance, passive targeting or enhanced permeability and retention (EPR) effect of nanoparticles enables the accumulation of its active ingredient in the tumour site [22]. In addition to site-specific targeting,

well-structured nanocarriers with a high drug payload and stimuli-triggered release of drugs are crucial towards preventing repeat drug dosing [23].

However, to prolonged drug blood circulation time, stimuli-responsive nanocarriers are know to mask the DOX activity in circulation which only become activated when triggered by stimuli [22], with physical and chemical stimuli such as temperature, light, ultrasonic, ionic, redox and enzymes have been employed in the delivery of chemotherapuetics [9]. Althought, pH-trigger stimuli are widely employed in the delivery of anticancer drugs taking advantage of the tumour microenvironment [22].

Currently, gold, liposomes and silver nanoparticles demonstrate increased plasma concentration and localization of the drugs at the targeted site [22]. Despite all these uniques advantages, most nanocarriers are non-biodegradable with poor loading capacity thus required multiples doses in order to deliver required concentration which could initiate systemic toxicity and immunogenic responses [22]. Hence, inorganic, biogenic and biodegradable materials are generally preferred due to toxicological concerns. Since most nanocarriers use in nanomedicine posses the ability to maintain the therapeutic dose level of a particular drug at the targeted point of interest with a sustained release concentration in the systemic circulation [9]. Although, our major concern is that most of the common carriers commercially available are synthetic from organic materials, which could have cumulative cytological effects on the biological system [24].

Calcium salt are found abundantly in sea-shell in form of calcium carbonate aragonite polymorph, which are currently employed in tissue regeneration and drug developments [25], [26]. Since calcium carbonate are biogenic and biodegradable in nature, its nanocrystals can be use in delivering bioactive proteins, hydrophilic and

hydrophobic drugs [24], [27]. Moreover, they exhibit high loading capacity with DOX and with other insoluble anticancer agents due to the hydrazone bond carbon linkage and porous nature of the CSNP [25], [28]. It was also demonstrated that CSNP-DOX is less cytotoxic when compared to the free-DOX on normal cells lines [29], [30]. However, the information on the kinetic release mechanism would provide a better understanding in predicting the possible toxicities of CSNP-DOX which is lacking is scientific literature.

In this study, CSNP-DOX complex was prepared using precipitation approach as applied in our previous studies [28], with the amine functional ending of DOX, structurally linked to the carboxyl end of the CSNP through a hydrazone bond to form the complex which dissociate in weak acidic microenvironment by pronation of carboxylic group ending of CSNP. The drug release kinetics of CSNP-DOX was determined via bio-analytic method developed with the pharmacokinetic parameters obtained to confirm that CSNP has the ability to regulate and prolong DOX in blood circulation. To the best of our knowledge, this work was the first study to develop a bioanalytical method which was used to determine the pharmacokinetics parameters of DOX from CSNP in dog's plasma circulation which has never been reported in scientific literature. Based on these results, biogenic CSNP polymorph can be use in the delivery of DOX sparing the life of cells in their physiological state in dogs to be given long-term repeated doses for therapeutic purposes.

2. Results

2.1 Cockleshell nanocarrier synthesis and characterization

The CSNP and CSNP-DOX produced have an average particle size of 28.0 ± 1.2 nm and 34.0 ± 3.4 nm in diameter respectively. CSNP and CSNP-DOX appears to be homogeneous and spherical in shape as shown in Figure 1, with a mean surface zeta

potential of – 19.2 mV and – 32.4 mV and polydispersity index of 0.132 and 0.312 respectively (Table 1). However, an encapsulation efficiency of 92.7% and a loading capacity greater than 70%.

2.2 Release kinetic studies

The DOX release kinetic from CSNP was evaluated using the snakeskin dialysis bag in phosphate buffer (pH 7.4) and citrate acid buffer (pH 4.8, 5.5 & 6.0) at 37 °C. The amount of DOX in the medium was determined based on a calibration curve (r^2= 0.991), Y = 5.998X + 0.129 Y absorbance, X = concentration (µg mL^{-1})] (Figure 2). It is important to note that initial burst release was observed at a faster rate within the first 4.5 hours (8%) followed by a slower sustained release at the remaining 8 days.

Free-DOX was used as a positive control in the release kinetic assay (Figure 3). At pH 7.4, the release of DOX from CSNP was sustained and relatively slows when compared to the free-DOX solution. About 52.6% (3.7 mg) of free-DOX was rapidly released in the first 96 hours, while only 13.7% (0.9 mg) of DOX was recorded from CSNP-DOX sample within the first 96 hours. The CSNP-DOX in acidic medium show a greater DOX release rate than in pH 7.4 in response to the pH change. In the first 96 hours, about 25% (1.8 mg) of DOX was detected, with an increasing rate of drug release over time as compared to the drug release pattern of CSNP carrier in the pH 7.4. The data generated were fitted into three different kinetic equations and according to the coefficient of determination (R^2), the Higuchi equation was best fitted compared to the first order and zero order regression models as shown in Table 2. In which the mechanism of DOX release is described by Higuchi equations; which mean that the release fashion is as a result of steady diffusion due to slow degradation of the nanoparticle as shown in figure 4.

2.3 General observation on feed intake, heart rate and haematology

There was a general decrease in feed consumption in the two groups after 24 hours intravenous administration of both free-DOX and CSNP-DOX. However, the heart rates during the period were within the normal range in both groups with no statistically significant changes were observed in the haematological profile within 48 hours with $p > 0.05$ in all of the parameters as shown in Table 3. All of the dogs were clinically healthy with no clinical evidence of systemic disturbance observed.

2.4 Analytical method development and validation

The method developed was optimized to reduce cross-matching using an organic solvent (acetonitrile HPLC grade) and buffer solution (pH 4.6) at different concentrations. Elution of the Chromatographs with the baseline at low wavelengths indicates that the method was selective for the detection of DOX with a clear resolution between DOX peak and that of the internal standard as shown in figure 5. The excellent extraction yield from the plasma was evident by the low interference from other protein molecules peaks on the chromatogram. The retention times observed for DOX and daunorubicin was 4.4 and 5.4 minutes respectively (Figure 5).

2.4.1 Linearity of calibration curve

A linear relationship was obtained from the concentration verse peak area ratio of 0.25 – 4 µg/mL with a coefficient of determination, slope and intercept value of 0.9973, 0.1253 and 0.0027 respectively (Figure 6).

2.4.2 Extraction recovery yield, Limit of detection, limit of quantification and coefficient of variation

The average recovery extraction was determined in triplicate of the blank plasma was 89.87% recovery from 1 µg/mL of DOX (Table 4). The limit of detection (LOD) of DOX at the ratio of 4:1 in the organic solvent was 549.90 ng/mL which corresponds to signal to noise of the method developed with a lower limit of quantification (LOQ) at 1666.0 ng/mL as shown in Table 5.

2.5 Doxorubicin plasma to whole blood partition fraction

Free-DOX has a significant higher fraction of DOX in plasma and red blood cells 1.862 ± 0.098 when compared the ratio of DOX partition from the CSNP-DOX (0.420 ± 0.004). This indicated a low rate of DOX release from the nanocarrier due to lack of external or environmental stimuli, which triggers the release from the pH sensitive material carrier.

2.6 Pharmacokinetics evaluation of free-DOX and CSNP-DOX in dogs

2.6.1 Animal dosing protocol and sample collection for plasma concentration determination

There was no evidence of any microbial growth upon incubation of the CSNP at 37 ^{o}C for 48 hours since all of the glassware used was sterile with the CSNP being stored at 50 ^{o}C in the oven. In addition, a sub-toxic dose (30 mg/m^2) was given to prevent any unwanted side effects such as vomiting and anaemia which could alter the results.

2.6.2 DOX plasma concentration and pharmacokinetics parameters

The mean plasma concentration-time data from both free-DOX and CSNPDOX administered to dogs are as shown in Table 6. The CSNP carrier tends to change the level of DOX concentration in systemic circulation when compared to the concentration in dogs given free-DOX. The level of DOX concentration decreases rapidly within first 4 hours after administration which goes below the LOD after 48 hours. Subsequently, the CSNP alters the pharmacokinetic parameter when compared to the group of dogs given free DOX. A substantial increase in the half-life ($t_{1/2}$), and area under the curve (AUC) were observed with CSNP-DOX which when compared to the free-DOX parameter, with an increase in the $t_{1/2,}$ with a 6 fold differences in the AUC. A significant wide volume of distribution of DOX (6.83 mg/(µg/mL) was demonstrated with free-DOX (3 times higher compared to the dogs given CSNP-DOX) with much more rapid clearance rate of 0.14 mg/(µg/mL) which is 3.5 times higher as compared to the dogs given CSNP–DOX as shown in Table 7. The DOX plasma concentration following single dose administration of CSNP-DOX was higher in all of the corresponding time intervals when compared to the dogs given free-DOX with a calculated bioavailability using the AUC values of CSNP-DOX against the free-DOX being 5.6% as shown in Table 7 below.

The retention time for DOX was 4.42 minutes with the highest plasma peak concentration at 26.75 ± 0.06 µg/mL and lowest plasma peak concentration at 2.22 ± 0.15 µg/mL as the lowest detectable concentration which is equivalent to the 13.6% of the DOX delivered as shown in figure 7.

3. Discussion

In this study, we hypothesized that CSNP is pH-stimuli responsive drug carrier that decompose in acidic microenivironment, which trigger the release of DOX in a slow

sustained release fashion. The characteristics of these nanocarriers are of great importance for stimuli trigger response and drug delivery. Here, we provide an amazing report on the *in vitro* kinetic release mechanism, bioanalytical method model and pharmacokinetics profile of CSNP-DOX in healthy dogs, which could ameliorate the narrow therapeutic index and poor selectively of DOX which have led to the use of nanocarriers in the attempt to improve the chemotherapeutic potential of DOX [14].

Unlike DOX alone, CSNP-DOX demonstrated a pH stimuli-responsive tool in *in vitro* release at acidic pH of 6.0 and below medium and encourages time-dependent DOX release from CSNP which could serve as basis for its application in anticancer delivery. Since, pH-triggered release is an essential tool for anticancer targeted delivery, with tumours possessing abundant lactic acid due to hypoxia [5], [7]. The percentage of DOX concentration release in the acidic pH medium when compared to the free-DOX in the neutral pH medium was quite adequate enough to elicit optimal therapeutic effect as earlier reported by [11]. The release pattern demonstrated by CSNP loaded with DOX was encouraging due to the sustained release fashion observed in the neutral pH, when compared to the release profile observed in pH 4.8 - 6.0 and free-DOX at physiological pH 7.4. This low pH dependent responsive release pattern expressed by CSNP could reduce the off targeted effects to proliferative healthy cells and improve selectivity of DOX to tumour cells. Furthermore, the low percentage release pattern recorded makes it an excellent nanocarrier when compared to the result of [11], who reported a higher percentage release pattern which could be attributed to the analytical methods employed. This further confirmed that the dialysis bag diffusion method is a more

accurate method for drug release kinetic assay as earlier suggested by [31]. In addition, our findings were consistent with [8], [41] who found that the release profile of encapsulated drugs on nanocarriers depends on the environment of the receiving medium in which the nanocarrier is suspended.

As expected, the CSNP retained DOX at the neutral pH and rapidly released the drug upon triggering by weak acidic pH in a similar release pattern as reported by [33]. This suggest that DOX are bonded to the carrier by polyelectrolyte ion and Schiff's base linker which are easily separated in acidic pH medium due to deprotonation of the amine and carboxyl group ending. In addition, [34] and [35], also reported that proton donation as a result of pH interaction leading to ionic bond dissociation and degradation/decomposition of the nanocarrier, which eventually leads to drug release for pharmacological activity.

Liu et al. [9], works further clarify that, dimethylamine ions ($(CH_3)_2NH_2^+$) complex formed by nitrogen-carbon bond (hydrazone group), which when hydrolyzed in acidic conditions, from esters liberate DOX to the microenvironment. Vijayakameswara et al. [36], stated that the end amine functional group on DOX are sensitive to pH changes, causing dissociation of DOX from the carboxylic endings on drug carriers. These explanations suggest that inorganic aragonite CSNP can be used as a targeted smart nanocarrier in chemotherapy, since it could prolong DOX in blood circulation thus, prevents adverse side effects to proliferating healthy cells as seen with conventional therapy. However, the desorption process of CSNP was very slow which directly affect the dissolution rate, thus agrees with the reports of Svenskaya et al. [37].

The release kinetics pattern gives an inside view of the pharmacokinetic nature of the nano-drug formulation [38]. The slow release observed could be unconnected to slow degradability of the CSNP in the simulated mediums, which is an added advantage to the DOX release from the carrier molecules, when compared to the release profile in acidic medium. The smart pH-responsive control release demonstrated by the CSNP is a proof of its potential as an ideal nanocarrier for delivering anticancer drugs as earlier suggested by Wu et al. [39] & Zhou et al. [40]. However, when the rate of drug release is slow from the nanocarrier, tends to alter the drug pharmacokinetics which further offer a unique advantage towards the safety of the anticancer drug on prolifereating healthy cells as earlier reported by Peng et al. [41].

Drug release kinetics are influenced by many factors including the polymer matrix structure, degradation of the polymer matrix, drug diffusion and carrier geometry (Shaikh et al., 2015). The dissociation of DOX from CSNP follows the Higuchi mathematical kinetic model which describe drug release pattern from the carrier particles as reported by Shaikh et al. [42]. This study agrees with Shaikh et al. [42], that, a carrier matrix with porous nature at the nanoscale, typically release its payload drugs according to the Higuchi mathematical model thus explains the degradability of the nanocarrier in the receiving medium.

However, it is essential to empirically develop a bioanalytical method for the detection and quantification of analytes in biological samples. The benefit of the method developed in this study, is that it tends to reduce the use of toxic solvents in the extraction process and detection assay and associated with excellent selectivity when compared to several other published methods [43]–[45].

Many of the methods developed previously for DOX recovery from the drug carrier in plasma required the use acidic solvents [43], [44]. In comparison, the extraction method developed in this study could easily separate DOX from the sphere matrix of CSNP and from plasma protein with less acidic solvent combination. Conversely, in the preliminary studies, we observed that detection of DOX was not possible without buffering the mobile phase with an acid buffer at pH 4.7. Consequently, the method was validated in accordance with the ICH and bioanalytical method guidelines [46]. The application of liquid-liquid precipitation method has the ability to recover approximately 80% of DOX, which comparable with the earlier method developed by Dharmalingam and Nadaraju [44], though with less acidic solvent.

The accuracy of the method developed was within the acceptable range of the coefficient of variation by the standard of USFDA bioanalytical method for HPLC, since it did not exceed 15% in all triplicate samples used in the validation assessment. In addition, this method possesses excellent ability to separate and detect DOX without interference of similar structural metabolites such as daunorubicin and another analyte present in the plasma due to the distinct differences in their retention times. Although, other scholars used fluorescent detectors in for detecting DOX [47]–[49], the selectivity of our method aided in specific detection and quantification of DOX devoid of other chromatographic peaks. However, the method used was unable to detect very low concentrations that are less than 500 ng/mL, though this is concentration is insignificant in clinical application in dogs [39]. The method developed uses simple precipitation techniques, with a linearity that possesses a wide limit of concentration and was reproducible using a simple, easily prepared mobile

phase with a short run time, making it applicable for quantification of DOX concentration for pharmacokinetic studies from dog's plasma.

DOX concentration in plasma to whole blood cells proportion ratio has a great significant importance in pharmacokinetics, with DOX in plasma to blood cells ratio describing the distribution of DOX in circulation within the plasma and blood cells. The dose selection used were on the basis of DOX toxicity in dogs as earlier reported by Baldwin et al. [50].

The result of free DOX plasma concentration was consistent with that of Niu et al. [51], that free-DOX are rapidly cleared from the plasma circulation with little seen in tissues. However, variations in the plasma concentration and half-life and other pharmacokinetic parameters are strongly dependent on the sensitivity of the bioanalytical method employed in detection the analytes [52]. The differences in the pharmacokinetic parameters of free DOX and conjugated DOX were similar to the earlier report of Li and Huang [20] on the kinetics profile of free DOX compared to the entrapped DOX on transporter nanocarrier in the treatment of cancer in rats model. Likewise, the report of Shah [53], agrees with the half-life and plasma concentration maximum observed in this study for free-DOX showing a high concentration on DOX in plasma when compared to the encapsulated DOX administered in healthy dogs. The low plasma concentration obtained from CSNP-DOX was a direct backwards phase process of the DOX incorporated in the matrixes which were released slowly into systemic circulation. These findings agree with the statement of Arias [34], that only drug released from the carrier matrix are quantified for pharmacokinetic analysis.

Moreover, the electrokinetics potential of the CSNP used as a carrier could have influenced the interaction process and the amount of DOX in circulation at each predetermined time point. Thus, agrees with earlier submission of Honary and Zahir [54], that pharmacokinetics of the drugs delivered are altered by the colloidal zeta potential of the delivery carrier.

The prolonged half-life recorded by CSNP-DOX in the dogs could be attributed to the slow release as earlier demonstrated by CSNP-DOX in neutral pH 7.4 in the *in vitro* release kinetics studies. The increased half-life observed with CSNP-DOX in the dogs when compared to the dogs given free-DOX could increase DOX potency and efficacy. Likewise, the prolonged circulation time demonstrated by CSNP incorporated with DOX is a good characteristic for a controlled nanocarrier with targeting ability. These findings concur with reports of Singh and Lillard [31], that when biodegradable materials are used in drug delivery, a very slow release fashion were demonstrated.

Similarly, the slow clearance rate was recorded with CSNP-DOX as when compared to the free-DOX. This was clearly attributed to the delayed release of the DOX from the nanoparticle which needs external stimuli, to trigger the release into the circulation. However, the low volume of distribution demonstrated were consistent with the reports of other scholars who use polymers in the delivery of DOX in the absence of triggering stimulus that causes the release of DOX encapsulated in the CSNP [55].

Furthermore, a significant increase in the half-life, AUC, and decrease in the volume of distribution and clearance rate of DOX conjugated to the CSNP were consistent with the report of Lu et al. [56], who documented increase of pharmacokinetic

parameters as a result of incorporation of DOX to micelles carrier when compared to the parameters of free-DOX. These alterations in C_{max} and half-life of DOX incorporated on CSNP agrees with the findings of Giodini et al. [57] as pharmacokinetics parameters are essential parameters for improving the therapeutic index. In addition, cytarabine and docetaxel loaded on CSNP in the mice and rats, with improved therapeutic efficacy in the treatment of acute leukaemia and breast cancer respectively [24].

However, not all of the changes in the pharmacokinetics parameters were solely due to the DOX properties. Some changes could be associated with the nanocarrier physiochemical properties as earlier cited by Caron et al.[58], who reported that the distribution of drugs depends on the properties of the carrier molecules. Several scholars consistently reported rapid clearance of DOX concentration in plasma of different animal models in less than 24 hours after administration [56], which is contrary to our findings when DOX is loaded to CSNP and administered intravenously in dogs. The low clearance rate associated with increased half-life observed in this study demonstrated prolonged circulation of DOX in the plasma.

4. Conclusion

In conclusion, CSNP loaded with DOX has influenced the retention of the DOX in blood circulation and enhances its bioavailability, which corresponds to the controlled and sustained release observed earlier in the *in vitro* release profile. The successful pH-triggered release of the CSNP-DOX suggests a promising potential of CSNP as a drug carrier conjugated with anticancer molecules for future clinical application. However, Hiquchi mathematical model best fits the kinetics release indicating a slow degradation of the CSNP in a physiological medium, with a simple

and rapid bioanalytical method was developed and applied in pharmacokinetics studies of CSNP-DOX in healthy dogs. Furthermore, the pharmacokinetic parameters confirm that CSNP has the ability to regulate and prolong DOX in blood circulation, thus translating to an improved pharmacological property of the DOX. Based on these results, CSNP may be useful in the delivery of DOX sparing the proliferating cells in their physiological state in dogs given long-term repeated doses of therapy.

5. Experimental (Materials and methods)

5.1 Drugs and reagents

Dodecyl dimethyl betaine (BS-12) were purchased from Sigma-Aldrich Co. (Sigma-Aldrich®, St. Louis, MO, USA). Deionized water was used as diluent which has a resistance of 18 MΩ taken from Milli R06 plus Q-Water system® (Organex, USA). HPLC grade acetonitrile and methanol, acetic acid, trifluoroacetic acid were purchased from Fisher Scientific (Fisher Scientific® UK). Doxorubicin hydrochloride (CAS No.: 25316-40-9) (purity 99.6%) with pH 5.13 and daunorubicin (CAS No: 23541-50-6) (purity 99.7%), were purchased from Beijing Mesochem Technology Co., Ltd. China. All other chemicals were of analytical grade and stored at 25 ^{o}C.

5.2 Synthesis, drug loading and characterization of CSNP and CSNP-DOX

Spherical aragonite CSNP was synthesized and characterized according to our previous work [28], Briefly, 2 g of the micro size cockleshell powder was precipitated in 50 mL of deionized water on a Telfon magnetic stirring machine at 1000 rpm for 1 hour at 25 ^{o}C. At the end of the preparation, the oven-dried nanoparticles (27 ^{o}C for 72 hours) were further processed on a ball mill (BML-2" Diahan Scientific® Korea) operated at 200 rpm for 48 hours before characterization. For the preparation of CSNP-DOX, a co-precipitation method was employed to incorporate DOX to the synthesized nanocarrier [28]. Characterization of the

synthesized nanocarrier and conjugated carrier for particle size, morphology and surface charge was done using High-resolution transmission electron microscopy (JEOL JEM 2100F HRTEM, Tokyo Japan) with an accelerating voltage of 100kV and Zetasizer ZS (Malvern, ver. 7.02 UK) with a scattering angle of 90̊ as done in our previous work [28].

5.3 *In vitro* drug release

The *in vitro* drug release assay was conducted using 0.01 M phosphate buffer pH 7.4 and citric sodium citrate acid medium pH 4.8, 5.5 and 6.0 to simulate physiological microenvironment, tumour stroma microenvironment and endosomal of cancer cell respectively. CSNP containing 7.2 mg DOX was aliquoted into 1 mL of phosphate buffer before dispensed into a snakeskin® dialysis tube (10 kDa, MWCO, Thermo Scientific®, USA), then suspended in 20 mL of pH 7.4, pH 4.8, 5.5 and 6.0 buffers solution respectively. A free-DOX solution containing 7.2 mg DOX was established in a similar manner without CSNP in accordance to the method of [59]. The CSNP-DOX and free-DOX in the dialysis systems were constantly stirred on Telfon magnetic stirrers at 100 rpm and 37 ± 0.5 ºC. At different time intervals (0, 0.3, 0.5, 1.0, 2.0, 3.0, 5.0, 8.0, 24.0, 48.0, 72.0, 96.0, 120.0, 144.0, 168.0, 192.0 hours), 1 mL aliquot was withdrawn from the systems for analysis which was immediately replaced with an equal volume of fresh solvent medium. The experiment was done in triplicate and analyzed using the zero-order equation, first order equation and Higuchi equation as described by [60], [61]. The data were presented in mean ± SD.

5.4 Analysis of doxorubicin concentration

A reverse-phase HPLC was used to detect DOX concentration release as described by Lu et al. (2015). The HPLC system consists of Separation Module 2690 from Water Corp. (Milford, MA USA) with a stationary phase of Agilent Eclipse C_{18}

Column (4.6 mm x 250 mm, 5 µm) (Santa Cala, CA, USA). The mobile phase was run with in a combination of mobile phase A (methanol) and B (0.1% acetic acid) at a flow rate of 1 mL/minute. The mobile phase was increased linearly from 40% to 90% in 5 minutes, followed by maintaining at 95% for 3 minutes and immediately returns to 40% composition in 1 minute. The system was further maintained for 4 minutes before the introduction of the subsequent sample, thus making a total run of 13 minutes at 30 ^{o}C. A photodiode array detector (Waters W2998, Milford, MA, USA) was set at a wavelength of 254 nm to detect DOX. Samples were analyzed in triplicate at an injection volume of 80 µL using Empower™ version 2 software.

For the pharmacokinetic study, daunorubicin was used as the internal standard (IS) of the DOX release. The above-mentioned HPLC settings were applied for pharmacokinetic study of CSNP-DOX except for the changes in the mobile phase. The HPLC system was run using mobile phase C (acetonitrile + 0.1% acetic acid) and D (0.1M disodium citrate acid pH 4.7). The mobile phase follows a linear gradient: mobile phase C increases from 40% to 60% in 5 minutes, then to 70% in 5 minutes and maintained for 5 minutes then returns to 60% for 4 minutes and finally returns to the initial mobile phase status after 1 minute.

5.4.1 Preparation of stock solution internal standard and quality control

One mg/mL of DOX and daunorubicin stock solutions were prepared using blank plasma while DOX aqueous solutions of 1.25 - 2.5 µg/mL range for quality control and 0.25 - 4 µg/mL for linearity were used. IS 1 µg/mL was included in all the samples before extraction process were performed on the plasma. The standard calibration curve of DOX was generated from the signal ratio of DOX to daunorubicin against the concentration of DOX. A DOX of 2 µg/mL and 0.25 µg/mL was used as the upper and lower quality control.

5.4.2 Method validation

The percentage recovery, lowest limit of detection (LOD) and lowest limit of quantification (LOQ) were determined from the ratio of the calibration curve slope and recovery percentage DOX. The validation of the method was conducted according to the international council of harmonisation (ICH) and bioanalytical method guideline [46]. The selectivity of the protocol was determined by using blank plasma from 3 healthy dogs spiked on DOX and daunorubicin to check where the chromatographic peak interloped with that of the extraction solvent.

5.4.3 Extraction of DOX and Daunorubicin from plasma

The extraction of the drugs from the plasma was performed using liquid-liquid extraction method. Briefly, 400 µL of acetonitrile: trifluoroacetic acid (95:5 v/v) was spiked to 99 µL of blank plasma from clinically healthy dogs with 1 µL of the IS. The mixture was then vortexed vigorously for 3 minutes and centrifuged at 5000 x g for 15 minutes at 18 ^{o}C (Eppendorf® 5424r, Germany). 200 µL of the supernatant was transferred into HPLC inserts for analysis with the blank plasma was used as a control for the analysis. The extraction yield was evaluated at a low DOX concentration within the limit of 0.25 to 4 µg/mL.

$$\text{Extraction yield} = \frac{\text{Peak area of DOX in blank plasma}}{\text{Peak area of DOX in acetonitrile}} \times 100$$

5.5 Doxorubicin plasma concentration to blood partition

The affinity of CSNP-DOX to whole blood and plasma were determined according to the method of [62]. The protocol is determined by calculating the ratio of plasma to blood DOX concentration which is used to predict the distribution and clearance rate of the DOX-loaded on CSNP as compared to the free-DOX. Briefly, 10 µg/mL (50 µL) of the DOX and its CSNP-DOX (equivalent) were spiked into the 450 µL of

whole blood separately and were incubated at 37 °C for 1 hour. The samples were centrifuged at 5000 x g for 15 minutes at 18 °C to separate the plasma from the cells. DOX was extracted from the plasma and analyzed by the established bio-analytical method.

5.6. Animal dosing protocol and sample collection

Six healthy male canine (*Canis familiaris)* aged 9 – 36 months (mean 24.84 ± 6.6 months), weighing 10.00 – 16.30 kg (mean, 13.89 ± 1.60 kg) were acclimatized in the research facility at the Faculty of Veterinary Medicine, Universiti Putra Malaysia (UPM). The dogs were examined physically and clinically evaluated for their general health status. All procedures involving animal care and use were approved by the Institutional Animal Care and Use Committee (IACUC) of Universiti Putra Malaysia (UPM/IACUC/AUP-RO13/2016). Microbiological assessment of the synthesized nanoparticles was evaluated before DOX were loaded and intravenously administered. This was done by direct inoculation of 400 µL of the nanoparticles on a general purpose medium (nutrient agar) and was incubated for 72 hours at 37 °C after which microorganism growth on the media was examined.

All dogs were chemotherapeutic naive for 2 weeks prior to the experiment. The dogs were fasted overnight prior to the experiment and fed 3 - 4 hours after the administration of DOX and CSNP-DOX. Three dogs were enrolled into group A which received CSP-DOX at 30 mg/m^2 intravenously via cephalic vein over 3 – 10 minutes. The remaining 3 dogs were enrolled into group B and were given free-DOX at the dose of 30 mg/m^2 (1 mg/kg for dogs less 15 kg) through a side port on the intravenous administration line and all the two groups were supported with 0.9%

sodium chloride (NaCl); 18.0 mL/kg/h intravenously via cephalic vein over 5 – 10 minutes, which are similar to the dose rate given in clinical schedules.

Blood samples (3 mL) were collected from the cephalic vein using a 22 G, ½ "needle (Terumo®, Belgium) into heparinized ethylenediamine tetraacetic acid (EDTA) tubes for haematology and DOX plasma concentration quantification. The blood samples were collected at points 0, 0.2, 0.5, 1, 2, 4, 6, 12, 24, 48, 60 hours after drug administration and immediately centrifuged (10,000 x g for 15 mins at 18 °C) to separate the plasma. The blood samples were stored at -80 °C before analysis. The DOX plasma concentrations were determined using the developed protocol and HPLC method above.

5.6.1 Haematological analysis

The haematological analysis was done using an automated haema-analyzer (Scil® Vet ABC, USA) to procure the following parameters: white blood cells, red blood cells, haemoglobin concentration, haematocrit, mean corpuscular volume, mean corpuscular haemoglobin concentration and platelets.

5.7. Release kinetics and pharmacokinetics parameters

The results from the release kinetics were expressed as mean ± standard deviation from triplicate data. The pharmacokinetic parameters were calculated using non-compartmental IV infusion analysis with a PKSolver 2.0, Microsoft Excel add-in [63], which was validated in *Computer Methods and Programs in Biomedicine Journal* 2010. The following parameters were determined (i) maximum plasma concentration (C_{max}), (ii) time to C_{max} (T_{max}), (iii) the area-under-the-curve between 0 and 72 (AUC_{0-72}), (iv) Area-under-the-curve between 0 and ∞ ($AUC_{0-\infty}$) and (*v*) Apparent half-life in plasma ($t_{1/2}$) (vi) Mean residence time (MRT) (vii) Volume of

distribution at steady-state (Vss) (viii) Systemic clearance (Cl) (ix) Elimination rate constant (K). The relative bioavailability (Fr) was calculated according to the following equation:

$$Fr = AUCS/AUCR$$

Where AUCS(CSNP-DOX) and AUCR (free-DOX) are the $AUC_{0\text{-}72}$ of each sample.

Author's contributions

DA and ZA contributed in developing the composite, all evaluation and data analysis writing the manuscript; GTS and HCW contribute in the drug delivery and manuscript writing, MHMN and HCW contribute in the release kinetics assay and pharmacokinetic evaluation; ZA; GTS, MHMN, RM concise the original ideal of the work.

Funding

The work was financially supported by the Prototype Development Research Grant Scheme (PRGS 5532300) of the Malaysian Ministry of Higher Education and Usmanu Danfodiyo University Sokoto-Nigeria scholarly sponsorship award.

Competing interests

The authors declare that they have no competing interests.

References

[1] R. R. Castillo, M. Colilla, and M. Vallet-Regí, "Advances in mesoporous silica-based nanocarriers for co-delivery and combination therapy against cancer," *Expert Opin. Drug Deliv.*, vol. 5247, no. July, pp. 1–15, 2016.

[2] Z. Wang, Q. He, W. Zhao, J. Luo, and W. Gao, "Tumor-homing, pH- and ultrasound-responsive polypeptide-doxorubicin nanoconjugates overcome doxorubicin resistance in cancer therapy," *J. Control. Release*, vol. 264, pp. 66–75, 2017.

[3] J. Zhao, H. Yang, J. Li, Y. Wang, and X. Wang, "Fabrication of pH-responsive PLGA (UCNPs / DOX) nanocapsules with upconversion luminescence for drug delivery," *Sci. Rep.*, no. 2, pp. 1–11, 2017.

[4] Y. Ma *et al.*, "pH-responsive mitoxantrone (MX) delivery using mesoporous silica nanoparticles (MSN)," *J. Mater. Chem.*, vol. 21, no. 26, p. 9483, 2011.

[5] S. Dissanayake, W. A. Denny, S. Gamage, and V. Sarojini, "Recent developments in anticancer drug delivery using cell penetrating and tumor targeting peptides," *Journal of Controlled Release*, vol. 250. pp. 62–76, 2017.

[6] D. D. Gurav, A. S. Kulkarni, A. Khan, and V. S. Shinde, "pH-responsive targeted and controlled doxorubicin delivery using hyaluronic acid nanocarriers," *Colloids Surfaces B Biointerfaces*, vol. 143, pp. 352–358, 2016.

[7] A. Jhaveri, P. Deshpande, and V. Torchilin, "Stimuli-sensitive nanopreparations for

588 combination cancer therapy," *Journal of Controlled Release*, vol. 190. pp. 352–370, 2014.

589 [8] M. Karimi *et al.*, "pH-Sensitive stimulus-responsive nanocarriers for targeted delivery of
590 therapeutic agents," *Wiley Interdisciplinary Reviews: Nanomedicine and Nanobiotechnology*,
591 2016.

592 [9] J. Liu *et al.*, "PH-Sensitive nano-systems for drug delivery in cancer therapy," *Biotechnology*
593 *Advances*, vol. 32, no. 4. pp. 693–710, 2014.

594 [10] S. Hossen, M. K. Hossain, M. K. Basher, M. N. H. Mia, M. T. Rahman, and M. J. Uddin,
595 "Smart nanocarrier-based drug delivery systems for cancer therapy and toxicity studies: A
596 review," *Journal of Advanced Research*. 2019.

597 [11] A. Shafiu Kamba, M. Ismail, T. A. Tengku Ibrahim, and Z. A. B. Zakaria, "A pH-sensitive,
598 biobased calcium carbonate aragonite nanocrystal as a novel anticancer delivery system.,"
599 *Biomed Res. Int.*, vol. 2013, p. 587451, 2013.

600 [12] K. Chatterjee, J. Zhang, N. Honbo, and J. S. Karliner, "Doxorubicin cardiomyopathy,"
601 *Cardiology*, vol. 115, no. 2, pp. 155–162, 2010.

602 [13] F. Yang, W. Ai, F. Jiang, X. Liu, Z. Huang, and S. Ai, "Preclinical Evaluation of an
603 Epidermal Growth Factor Receptor-Targeted Doxorubicin-Peptide Conjugate: Toxicity,
604 Biodistribution, and Efficacy in Mice," *J. Pharm. Sci.*, vol. 105, no. 2, pp. 639–649, 2016.

605 [14] A. M. Rahman, S. W. Yusuf, and M. S. Ewer, "Anthracycline-induced cardiotoxicity and the
606 cardiac-sparing effect of liposomal formulation," *International Journal of Nanomedicine*, vol.
607 2, no. 4. pp. 567–583, 2007.

608 [15] Y. Ichikawa *et al.*, "Cardiotoxicity of doxorubicin is mediated through mitochondrial iron
609 accumulation," *J. Clin. Invest.*, vol. 124, no. 2, pp. 617–630, 2014.

610 [16] X.-P. Sun, L.-L. Wan, Q.-J. Yang, Y. Huo, Y.-L. Han, and C. Guo, "Scutellarin protects
611 against doxorubicin-induced acute cardiotoxicity and regulates its accumulation in the heart,"
612 *Arch. Pharm. Res.*, no. 600, pp. 1–9, 2017.

613 [17] Y. Zhang *et al.*, "Co-delivery of doxorubicin and curcumin by pH-sensitive prodrug
614 nanoparticle for combination therapy of cancer.," *Sci. Rep.*, vol. 6, no. February, p. 21225,
615 2016.

616 [18] J. L. Rowell, D. O. McCarthy, and C. E. Alvarez, "Dog Models of Naturally Occurring
617 Cancer," *Trends Mol. Med.*, vol. 17, no. 7, pp. 380–388, 2012.

618 [19] C. Weinz, T. Schwarz, D. Kubitza, W. Mueck, and D. Lang, "Metabolism and excretion of
619 rivaroxaban, an oral, direct factor Xa inhibitor, in rats, dogs, and humans.," *Drug Metab.*
620 *Dispos.*, vol. 37, no. 5, pp. 1056–64, 2009.

621 [20] S. D. Li and L. Huang, "Pharmacokinetics and biodistribution of nanoparticles," *Mol. Pharm.*,
622 vol. 5, no. 4, pp. 496–504, 2008.

623 [21] N. Jia *et al.*, "Preparation and evaluation of poly(L-histidine) based pH-sensitive micelles for
624 intracellular delivery of doxorubicin against MCF-7/ADR cells," *Asian J. Pharm. Sci.*, vol.
625 12, no. 5, pp. 433–441, 2017.

626 [22] W. Zhang *et al.*, "Centromere and kinetochore gene misexpression predicts cancer patient
627 survival and response to radiotherapy and chemotherapy.," *Nat. Commun.*, vol. 7, no. May, p.
628 12619, 2016.

629 [23] N. Tang, G. Du, N. Wang, C. Liu, H. Hang, and W. Liang, "Improving penetration in tumors
630 with nanoassemblies of phospholipids and doxorubicin," *J. Natl. Cancer Inst.*, vol. 99, no. 13,
631 pp. 1004–1015, 2007.

[24] A. Danmaigoro, G. T. Selvarajah, M. H. Mohd Noor, R. Mahmud, and M. Z. Abu Bakar, "Toxicity and Safety Evaluation of Doxorubicin-Loaded Cockleshell-Derived Calcium Carbonate Nanoparticle in Dogs," *Adv. Pharmacol. Sci.*, 2018.

[25] N. I. Hammadi *et al.*, "Formulation of a Sustained Release Docetaxel Loaded Cockle Shell-Derived Calcium Carbonate Nanoparticles against Breast Cancer," *Pharm. Res.*, vol. 34, no. 6, pp. 1193–1203, 2017.

[26] A. Z. Jaji, Z. Bin, A. Bakar, and R. Mahmud, "Synthesis , characterization , and cytocompatibility of potential cockle shell aragonite nanocrystals for osteoporosis therapy and hormonal delivery," pp. 23–33, 2017.

[27] A. Z. Jaji *et al.*, "Safety assessments of subcutaneous doses of aragonite calcium carbonate nanocrystals in rats," *J. Nanoparticle Res.*, vol. 19, no. 5, p. 175, 2017.

[28] A. Danmaigoro *et al.*, "Development of Cockleshell (Anadara granosa) Derived CaCO 3 Nanoparticle for Doxorubicin Delivery," 2017.

[29] W. Fu *et al.*, "In vitro evaluation of a novel pH sensitive drug delivery system based cockle shell-derived aragonite nanoparticles against osteosarcoma," *J. Exp. Nanosci.*, vol. 8080, no. March, pp. 1–22, 2017.

[30] D. L. Gustafson and D. H. Thamm, "Pharmacokinetic modeling of doxorubicin pharmacokinetics in dogs deficient in ABCB1 drug transporters," *J. Vet. Intern. Med.*, vol. 24, no. 3, pp. 579–586, 2010.

[31] R. Singh and J. W. Lillard, "Nanoparticle-based targeted drug delivery," *Experimental and Molecular Pathology*, vol. 86, no. 3. pp. 215–223, 2009.

[32] S. E. McNeil, "Unique benefits of nanotechnology to drug delivery and diagnostics," *Methods Mol Biol*, vol. 697, pp. 3–8, 2011.

[33] J. Zhang *et al.*, "Calcium Carbonate Nanoplate Assemblies with1. Zhang J, Li Y, Xie H, et al. Calcium Carbonate Nanoplate Assemblies with Directed High-Energy Facets: Additive-Free Synthesis, High Drug Loading, and Sustainable Releasing. ACS Appl Mater Interfaces. 2015;7(29," *ACS Appl. Mater. Interfaces*, vol. 7, no. 29, pp. 15686–15691, 2015.

[34] J. L. Arias, "Drug Targeting by Magnetically Responsive Colloids," *Handb. Drug Target. Monit.*, pp. 19–111, 2010.

[35] Y. Liu, W. Wang, J. Yang, C. Zhou, and J. Sun, "pH-sensitive polymeric micelles triggered drug release for extracellular and intracellular drug targeting delivery," *Asian J. Pharm. Sci.*, vol. 8, no. 3, pp. 159–167, 2013.

[36] V. Vijayakameswara Rao, S. R. Mane, A. Kishore, J. Das Sarma, and R. Shunmugam, "Norbornene derived doxorubicin copolymers as drug carriers with pH responsive hydrazone linker," *Biomacromolecules*, vol. 13, no. 1, pp. 221–230, 2012.

[37] Y. Svenskaya *et al.*, "Anticancer drug delivery system based on calcium carbonate particles loaded with a photosensitizer," *Biophys. Chem.*, vol. 182, pp. 11–15, 2013.

[38] M. Jarosz, A. Pawlik, M. Szuwarzyński, M. Jaskuła, and G. D. Sulka, "Nanoporous anodic titanium dioxide layers as potential drug delivery systems: Drug release kinetics and mechanism," *Colloids Surfaces B Biointerfaces*, vol. 143, pp. 447–454, 2016.

[39] J. L. Wu, C. Q. Wang, R. X. Zhuo, and S. X. Cheng, "Multi-drug delivery system based on alginate/calcium carbonate hybrid nanoparticles for combination chemotherapy," *Colloids Surfaces B Biointerfaces*, vol. 123, pp. 498–505, 2014.

[40] T. Zhou, X. Zhou, and D. Xing, "Controlled release of doxorubicin from graphene oxide based charge-reversal nanocarrier," *Biomaterials*, vol. 35, no. 13, pp. 4185–4194, 2014.

[41] C. Peng, Q. Zhao, and C. Gao, “Sustained delivery of doxorubicin by porous CaCO3 and chitosan/alginate multilayers-coated CaCO3 microparticles,” *Colloids Surfaces A Physicochem. Eng. Asp.*, vol. 353, no. 2–3, pp. 132–139, 2010.

[42] H. K. Shaikh, R. V Kshirsagar, and S. G. Patil, “Mathematical Models for Drug Release Characterization : a Review,” *World J. Pharm. Pharm. Sci.*, vol. 4, no. 4, pp. 324–338, 2015.

[43] D. L. Chin, B. L. Lum, and B. I. Sikic, “Rapid determination of PEGylated liposomal doxorubicin and its major metabolite in human plasma by ultraviolet-visible high-performance liquid chromatography,” *J. Chromatogr. B Anal. Technol. Biomed. Life Sci.*, vol. 779, no. 2, pp. 259–269, 2002.

[44] S. R. Dharmalingam and S. Nadaraju, “A Simple HPLC Bioanalytical Method for the Determination of Doxorubicin Hydrochloride in Rat Plasma : Application to Pharmacokinetic Studies,” *Trop. J. Pharm. Res.*, vol. 13, no. March, pp. 409–415, 2014.

[45] M. M. Usman, “A fast and simple HPLC-UV method for simultaneous determination of three anti-cancer agents in plasma of breast cancer patients and its application to clinical pharmacokinetics,” *African J. Pharm. Pharmacol.*, vol. 5, no. 7, pp. 915–922, 2011.

[46] ICH, “Guidance for industry: Q2B validation of analytical procedures: methodology,” *Int. Conf. Harmon. Tech. Requir. Regist. Tripart. Guidel.*, no. November, p. 13, 1996.

[47] P. de Bruijn *et al.*, “Determination of doxorubicin and doxorubicinol in plasma of cancer patients by high-performance liquid chromatography.,” *Anal. Biochem.*, vol. 266, no. 2, pp. 216–221, 1999.

[48] J. Van Asperen, O. Van Tellingen, and J. H. Beijnen, “Determination of doxorubicin and metabolites in murine specimens by high-performance liquid chromatography,” *J. Chromatogr. B Biomed. Appl.*, vol. 712, no. 1–2, pp. 129–143, 1998.

[49] W. Shao, P. Arghya, M. Yiyong, L. Rodes, and S. Prakash, “Carbon Nanotubes for Use in Medicine : Potentials and Limitations,” *Synth. Appl. Carbon Nanotub. Their Compos.*, p. 28, 2013.

[50] J. R. Baldwin, B. A. Phillips, S. K. Overmyer, N. Z. Hatfield, and P. K. Narang, “Influence of the cardioprotective agent dexrazoxane on doxorubicin pharmacokinetics in the dog.,” *Cancer Chemother. Pharmacol.*, vol. 30, no. 6, pp. 433–8, 1992.

[51] Y. Niu, F. J. Stadler, J. Song, S. Chen, and S. Chen, “Facile fabrication of polyurethane microcapsules carriers for tracing cellular internalization and intracellular pH-triggered drug release,” *Colloids Surfaces B Biointerfaces*, vol. 153, pp. 160–167, 2017.

[52] G. Tiwari and R. Tiwari, “Bioanalytical method validation: An updated review,” *Pharm. Methods*, vol. 2, no. 1, p. 25, 2010.

[53] S. Shah, “Novel drug delivery carrier: Resealed erythrocytes,” *Int. J. Pharma Bio Sci.*, vol. 2, no. 1, pp. 394–406, 2011.

[54] S. Honary and F. Zahir, “Effect of zeta potential on the properties of nano-drug delivery systems - A review (Part 1),” *Trop. J. Pharm. Res.*, vol. 12, no. 2, pp. 255–264, 2013.

[55] L. M. Kaminskas *et al.*, “A comparison of changes to doxorubicin pharmacokinetics, antitumor activity, and toxicity mediated by PEGylated dendrimer and PEGylated liposome drug delivery systems,” *Nanomedicine Nanotechnology, Biol. Med.*, vol. 8, no. 1, pp. 103–111, 2012.

[56] J. Lu *et al.*, “Targeted Delivery of Doxorubicin by Folic Acid-Decorated Dual Functional Nanocarrier,” *Mol. Pharm.*, vol. 11, no. 11, pp. 4164–4178, 2015.

[57] L. Giodini *et al.*, “Nanocarriers in cancer clinical practice: a pharmacokinetic issue,”

722 *Nanomedicine Nanotechnology, Biol. Med.*, 2016.

723 [58] W. P. Caron, K. P. Morgan, B. a. Zamboni, and W. C. Zamboni, "A review of study designs
724 and outcomes of phase I clinical studies of nanoparticle agents compared with small-molecule
725 anticancer agents," *Clin. Cancer Res.*, vol. 19, no. 12, pp. 3309–3315, 2013.

726 [59] A. Fritze *et al.*, "Remote loading of doxorubicin into liposomes driven by a transmembrane
727 phosphate gradient," *Biochim. Biophys. Acta - Biomembr.*, vol. 1758, pp. 1633–1640, 2006.

728 [60] V. Cojocaru *et al.*, "Formulation and evaluation of in vitro release kinetics of na3cadtpa
729 decorporation agent embedded in microemulsion-based gel formulation for topical delivery,"
730 *Farmacia*, vol. 63, no. 5, pp. 656–664, 2015.

731 [61] K. Derakhshandeh, M. Soheili, S. Dadashzadeh, and R. Saghiri, "Preparation and in vitro
732 characterization of 9-nitrocamptothecin-loaded long circulating nanoparticles for delivery in
733 cancer patients.," *Int J Nanomed*, vol. 5, pp. 463–71, 2010.

734 [62] S. Pawar, G. Shevalkar, and P. Vavia, "Glucosamine-anchored doxorubicin-loaded targeted
735 nano-niosomes: pharmacokinetic, toxicity and pharmacodynamic evaluation," *J. Drug*
736 *Target.*, no. August, pp. 1–14, 2016.

737 [63] Y. Zhang, M. Huo, J. Zhou, and S. Xie, "PKSolver : An add-in program for pharmacokinetic
738 and pharmacodynamic data analysis in Microsoft Excel," *Comput. Methods Programs*
739 *Biomed.*, vol. 99, no. 3, pp. 306–314, 2010.

740

741 **Figures**

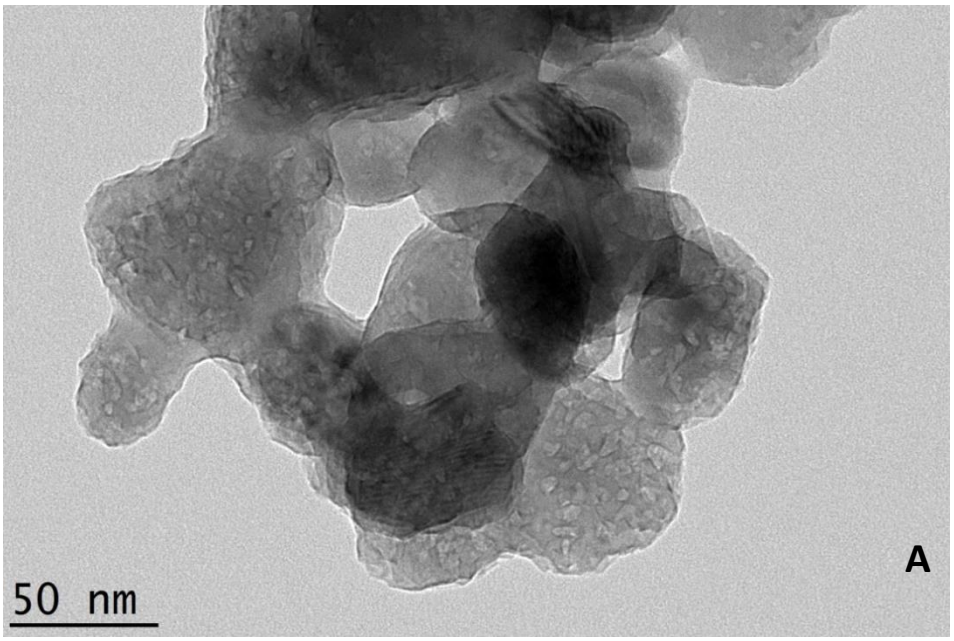

742

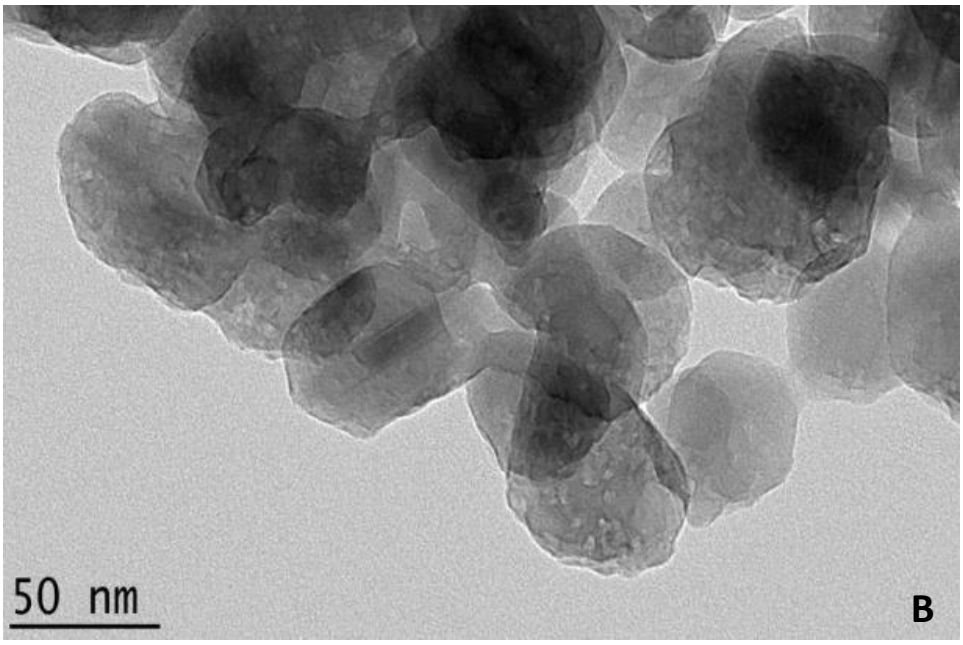

Figure 1: Electron micrograph of A) CSNP and B) CSNP-DOX. The porous particle appeared to be spherical in shape with an average size of 28 ±1.2 nm for CSNP and 34.0 ± 3.4 nm CSNP-DOX

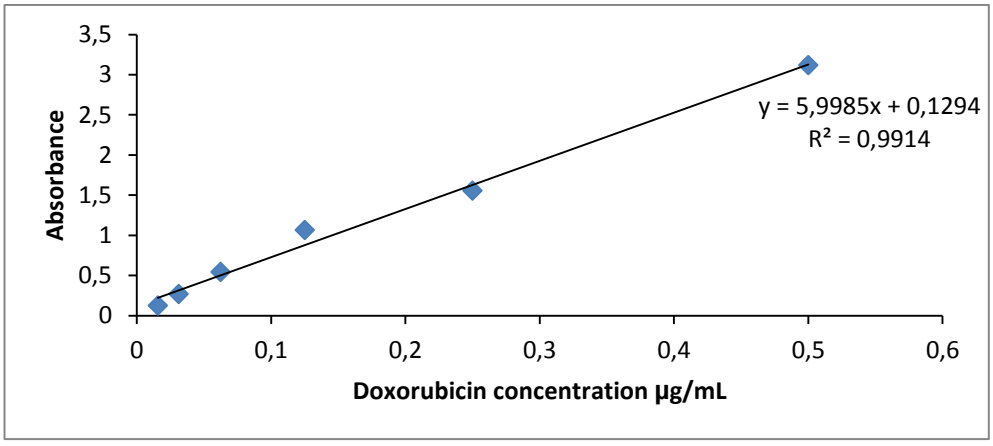

Figure 2: Calibration curve of DOX

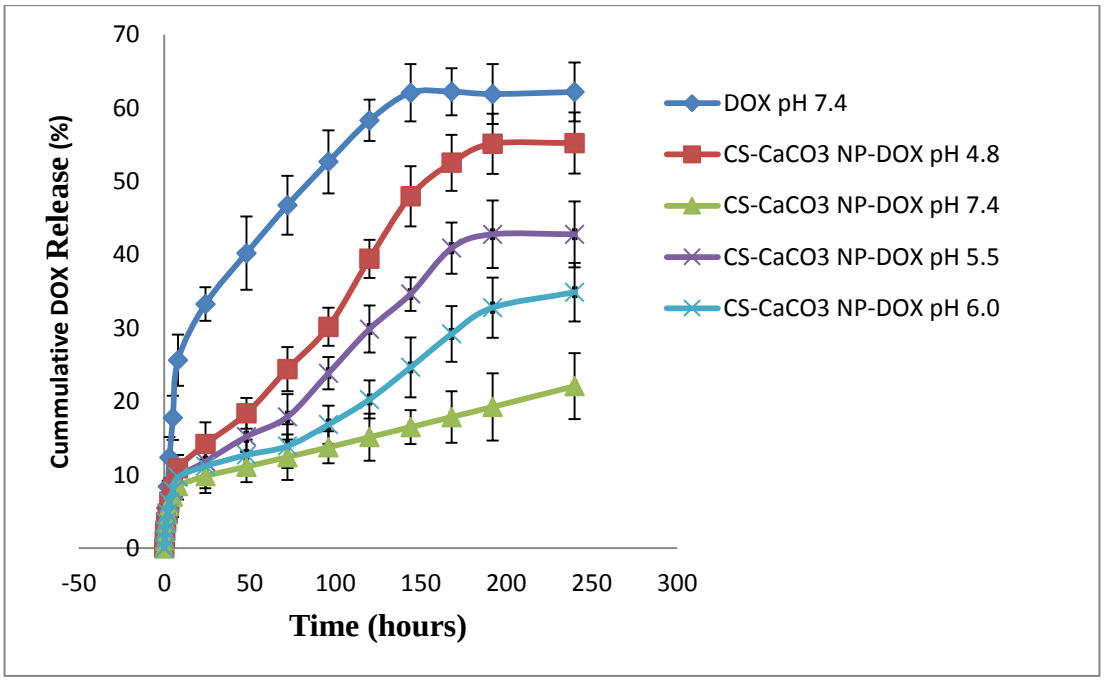

752

753 **Figure 3: The Cumulative release of free-DOX and CSNP–DOX, in *in-vitro* release kinetic in**
754 **different acidic and physiological pH medium. Triplicate data of each time point and value**
755 **analysis as mean ± SD, (n = 3)**

756

757

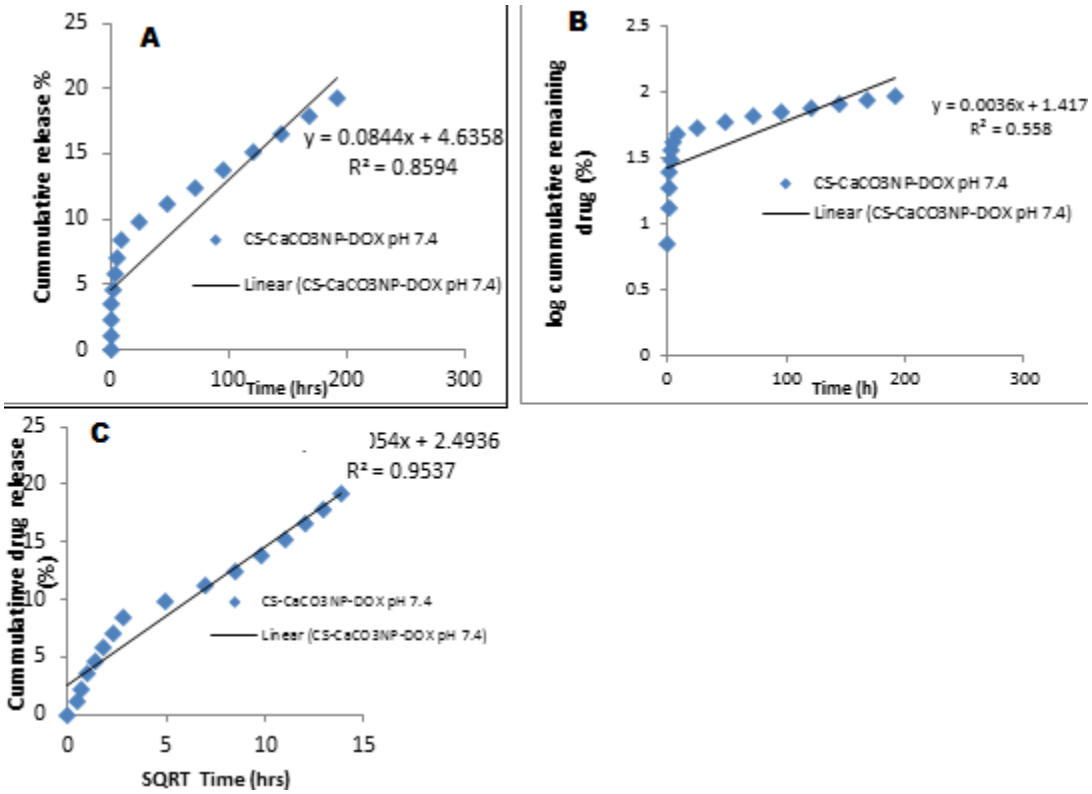

758

Figure 4: The kinetic release model of CSNP-DOX in pH 7.4 medium (A) Zero order kinetics release model of CSNP-DOX (B) First order kinetic release model of CSNP-DOX (C) Higuchi order kinetic release model of CSNP-DOX

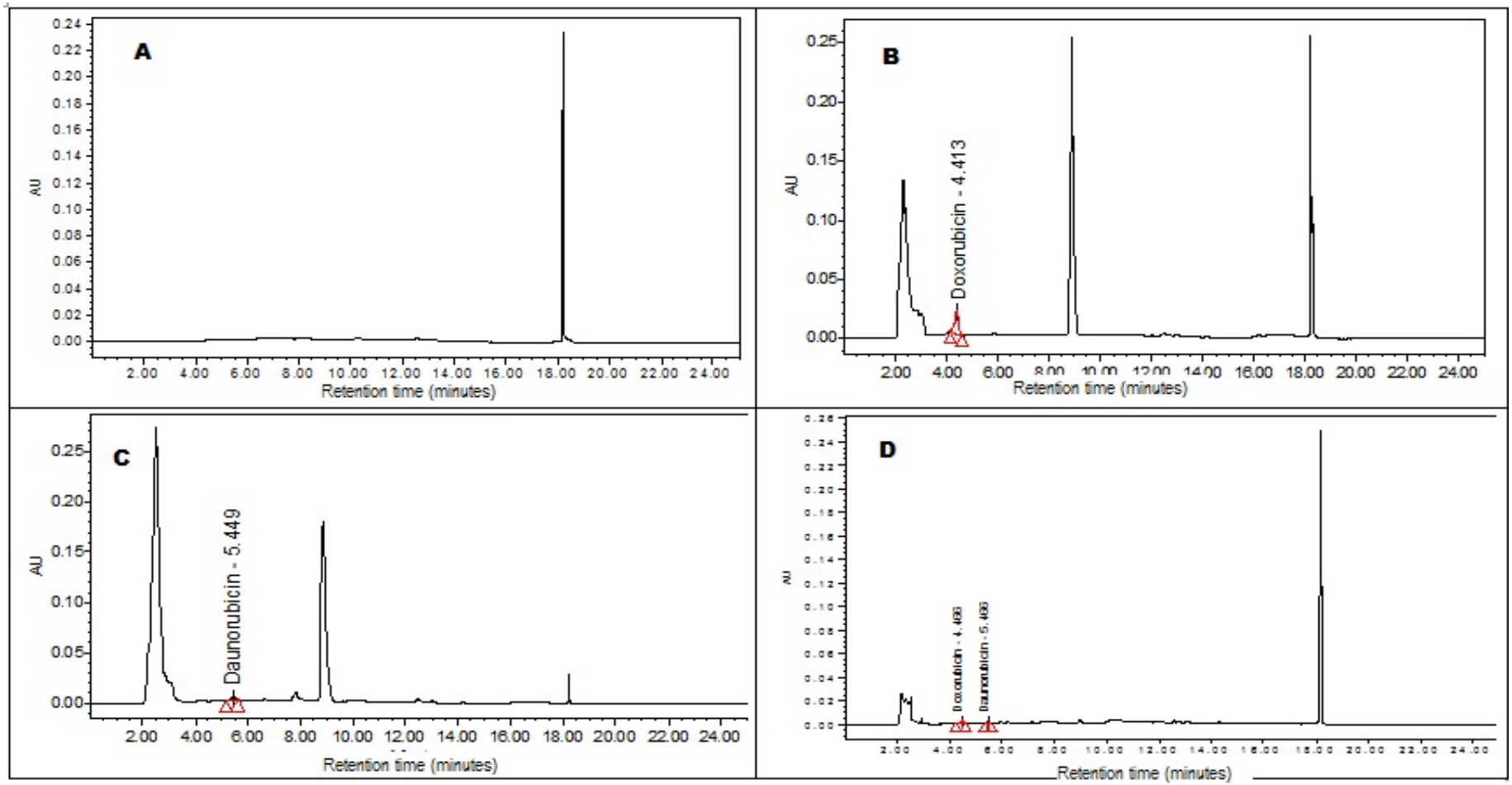

Figure 5: The chromatograms of blank plasma free-DOX, Daunorubicin (IS), DOX released from CSNP-DOX plasma from the canine. (A) Blank plasma from the canine (B) LLQ sample of DOX spiked on plasma (1.66 µg/mL), (C) Daunorubicin spiked on plasma (1.0 µg/mL), (D) Free-DOX release from CSNP-DOX after intravenous administration of 30 mg/m^2 at 60 hours

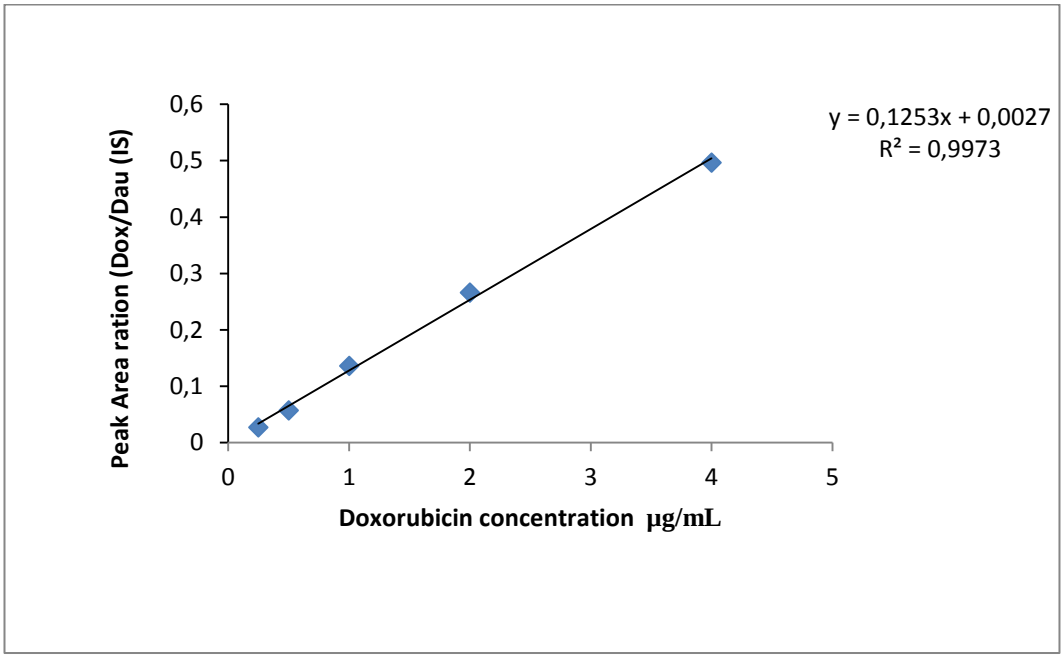

Figure 6: Linearity curve for the quantification of DOX from the peak ratio of DOX and daunorubicin

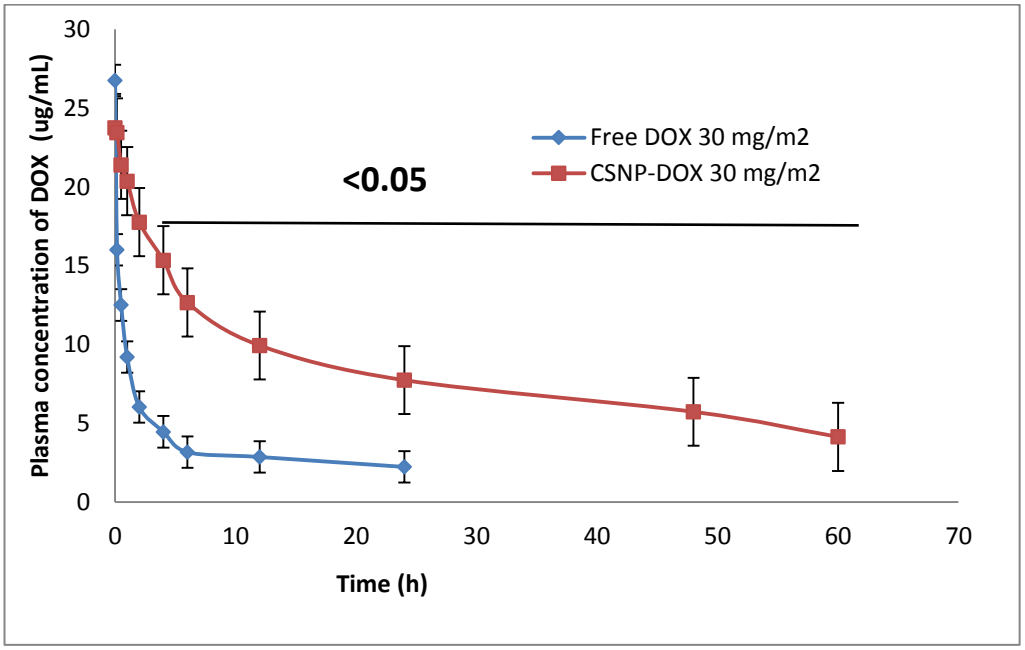

Figure 7: The plasma concentration time profile of DOX after free-DOX and CSNP-DOX i.v administration in dogs (n = 3) at a DOX dose 30 mg/m^2

Tables

Table 1: Physiocochemical properties of the CSNP and CSNP-DOX

Nanocarrier	Mean diameter size	Mean surface charge (mV)	Polydispersity index
CSNP	28.0 ± 1.2	- 19.2	0.132
CSNP-DOX	34.0 ± 3.4	- 32. 4	0.312

Table 2: Evaluation of the release kinetics based on zero order, first order and Higuchi equations

Coefficient of Determination (R^2)		
Zero order equation	**First order equation**	**Higuchi equation**
0.8594	0.5580	0.9537

Table 3: Haematological profile of free-DOX and CSNP-DOX single intravenous administration for pharmacokinetic studies in healthy dogs n = 3

	Free-Dox 30 mg/m^2 (n =3)			CSNP-DOX 30 mg/m^2 (n =3)		
Parameter	**0 hours**	**24hrs**	**48hrs**	**0 hours**	**24hrs**	**48hrs**
RBC 10^6/mm^3	7.08 ± 0.2	7.77 ± 0.1	5.82 ± 0.1	7.07 ± 0.32	7.1 ± 0.22	6.38 ± 0.2
HGB g/dl	15.07 ± 2	16.1 ± 1.5	14.4 ± 1.6	15.06 ± 1.59	14.1 ± 0.9	13.6 ± 0.8
HCT %	45.10 ± 5.3	46.8 ±3.8	48.4 ± 2.9	45.76 ± 3.84	42.5 ± 2.8	40.4 ± 2.2
MCV µm^3	64.00 ± 5.7	60 ± 4.8	64 ± 4.3	64 ± 4.0	60 ± 4.2	63 ± 3.6
MCH Pg	21.23 ± 2.2	20.7 ± 1.5	21.3 ± 1.4	21.23 ± 1.56	19.8 ± 0.9	21.3 ± 1.9
MCHC g/dl	33.40 ± 0.5	34.4 ± 0.2	33.5 ± 0.1	33.4 ± 0.44	33.2 ± 0.5	33.6 ± 0.3
RDW %	15.40 ± 0.3	14.6 ± 0.1	15.2 ± 0.1	15.4 ± 0.26	15.5 ± 0.3	15 ± 0.2
PLT 10^3/mm^3	233.33 ± 118	187 ± 9.0	178 ± 82	233.3 ±103.36	185 ± 99	163 ± 79.0
MPV µm^3	9.50 ± 1.4	10 ± 0.6	9.9 ± 1.0	9.5 ± 1.0	10.5 ± 0.9	10.7 ± 0.8
WBC 10^3/mm^3	9.10 ± 2.1	9.8 ± 1.8	10.6 ± 1.6	9.1 ± 2.71	8.9 ± 2.1	11.9 ± 2.8
LYM 10^3/mm^3	3.50 ± 0.9	4.2 ± 0.3	3.7 ± 0.1	3.5 ± 1.45	4.9 ± 0.2	4.1 ± 0.4
MON 10^3/mm^3	0.73 ± 0.1	1.0 ± 0.1	0.9 ± 0.1	0.73 ± 0.31	0.8 ± 0.2	1.2 ±0.1
GRA 10^3/mm^3	4.87 ± 2.9	5.6 ± 2.1	5.9 ± 2.0	4.86 ± 2.15	3.2 ± 1.5	6.6 ± 2.1
EOS 10^3/mm^3	0.32 ± 0.3	0.22 ± 0.1	0.34 ± 0.1	0.32 ± 0.1	0.14 ± 0.2	0.23 ± 0.2

All the values are expressed in mean and standard deviation, Student t-test analysis with $p < 0.05$ considered statistically significant.

Table 4: Percentage extraction yield of DOX from dog plasma

Concentration (µg/mL)	Calculated free DOX found (µg/mL)	Extraction recovery (%)
2.00	1.56	78.39
1.00	0.89	89.87
0.50	0.39	79.49
0.25	0.20	80.91

n = 6 for each sample concentration used for the analysis

Table 5: Analytical parameters of detection and quantification for the method developed for DOX quantification

Parameter	DOX
Concentration DOX added (µg/ml)	1.00
Mean SD	94.37 ± 11.01
Intercept (a)	0.002
Slope (b)	0.125
Correlation coefficient (r)	0.9973
Extraction recovery yield range (R%)	78.39 – 89.87
LOD (ng/mL)	549.96
LOQ (ng/mL)	1666.55
CV (%)	11.70

Where : LOD: Limit of detection; LOQ: Limit of quantification; CV: Coefficient of variation

Table 6: Plasma concentration values at different time interval for the two drug formulation from HPLC (n = 3) for each group

Time interval (h^{-1})	DOX (µg/mL)	CSNP-DOX (µg/mL)
0	26.75 ± 0.06	23.75 ± 1.35
0.16	16.0 ± 0.50	23.45 ± 1.22
0.5	12.50 ± 1.00	21.40 ± 2.22
1	9.20 ± 0.23	20.36 ± 2.10*
2	6.03 ± 0.13	17.76 ± 2.30*
4	4.45 ± 0.23	15.34 ± 1.90*
6	3.16± 0.40	12.66 ± 1.84*
12	2.85 ± 0.17	9.93 ± 0.93*
24	2.22 ± 0.15	7.73 ± 0.73*
48	-	5.72 ± 0.92*
60	-	3.93 ± 0.57*

Key: DOX: Doxorubicin, CSNP-DOX: Cockleshell derived nanoparticle loaded with doxorubicin and * < 0.05 which is considered statistical significant

Table 7: Pharmacokinetics parameters of CSNP-DOX and DOX alone following single dose 30 mg/m^2 intravenous administration (mean SD, n= 3) in dogs

Parameter	Unit	DOX	CSNP-DOX
$t_{1/2}$	H	30.96	35.59
T_{max}	H	0.00	0.00
C_{max}	µg/mL	26.75	23.75
AUC_{0-72}	µg/mL*h	87.84	495.03
AUMC	µg/mL*h^2	9130.29	33741.36
MRT	H	45.56	48.34
V_z	(mg)/(µg/mL)	7.57	2.21
Cl	(mg)/(µg/mL)/h	0.14	0.04
V_{ss}	(mg)/(µg/mL)	6.83	2.08
F	(mL/kg)	5.63	

Key: $t_{1/2}$: half-life; $T_{max:}$ Time at maximum concentration; C_{max}: Maximum concentration; AUC: Area under the curve; AUMC: Area under the first-moment curve; MRT: Mean residence time; V_z: Volume of distribution; Cl: Clearance rate; V_{ss}: Volume of steady distribution; F: Relative bioavailability